Preliminary study of phosphate adsorption onto cerium oxide nanoparticles for use in water purification. Nanoparticles synthesis and characterization

Sonia Recillas[a], Ana García[a], Edgar González[b], Eudald Casals[b], Victor Puntes[b,c], Antoni Sánchez[a*], Xavier Font[a]

a. Department of Chemical Engineering, Escola d'Enginyeria, Universitat Autònoma de Barcelona, 08193 Bellaterra, Spain.

b. Institut Català de Nanotecnologia, Campus de la Universitat Autònoma de Barcelona, 08193 Bellaterra, Spain.

c. Insitut Català de Recerca i Estudis Avançats, Passeig Lluís Companys, 23, 08010 Barcelona, Spain

*Corresponding author: E-mail: antoni.sanchez@uab.cat

Pre-print of: Recillas, S. et al. "Preliminary study of phosphate adsorption onto cerium oxide nanoparticles for use in water purification: nanoparticles synthesis and characterization" in Water science and technology,vol. 66, issue 3 (June 2012), p. 503-509. The final version is available at DOI 10.2166/wst.2012.185

Abstract

In this study, the synthesis and characterization of cerium oxide nanoparticles (CeO_2-NPs) and their adsorption potential for removing phosphate from water was evaluated using a multi-factor experimental design to explore the effect of various factors on adsorption. The objective function selected was the percentage of phosphate removed from water, in which the phosphate concentration and the CeO_2-NP concentration are quantitative variables (factors in the experimental design). A lineal polynomial fitted the experimental results well (R^2=0.9803). The nanostructure was studied by transmission electron microscopy and high-resolution transmission electron microscopy techniques before and after the adsorption process. During the adsorption and desorption processes several changes in the morphology and surface chemistry of the CeO_2-NPs were observed.

Keywords: cerium oxide nanoparticles; adsorption; desorption; phosphate; experimental design.

INTRODUCTION

Cerium nanoparticles (CeO_2-NPs) have been the subject of recent studies due to their applications in catalysis, fuel cells, optical films, and in other fields (Campbell and Peden, 2005; Yuan *et al.*, 2009). In recent years, promising results have been obtained in water treatment for chromium and arsenate removal by using CeO_2 nanoparticles or CeO_2 nanocomposites (Peng *et al*., 2005; Xiao *et al.*, 2009; Recillas *et al.*, 2010). Understanding the environmental process on a molecular level is key to several environmental processes (Al-Abadleh and Grassian, 2003). It is also important to evaluate the environmental impact after the complete adsorption-desorption process that occurs on the NPs. The NP synthesis conditions determine the specific adsorption behavior of the resultant NPs, because the redox properties can be modified, and their dual reversible reaction can modify the overall adsorption process.

Phosphate is a key contaminant in the eutrophication process (Fernández et al., 2003; Nowack and Stone, 2006; Laney et al., 2007). Therefore, the removal of phosphate from wastewater by chemical and biological treatments has been widely investigated; this usually results in complex biological operations or the production of chemical sludge (Barnard, 1983; Scheer and Seyfried, 1997). The adsorption and precipitation of phosphate by using fly ash and modified fly ash have been investigated in the search for economical adsorbents for phosphate (Xu *et al*., 2010). Nevertheless, the inconvenience of the precipitation process is that it requires a large amount of chemicals and produces a great deal of wastewater sludge (Ozacar, 2003). Even though the adsorption technique is useful and economical, only a few studies consider the recovery of the adsorbent used and the pollutant, which are crucial issues for the use of NPs in environmental processes where economics play a decisive role.

In the present study, a Box-Hunter spherical experimental design (Box *et al.*, 1978) and surface characterization techniques were used to study phosphate adsorption behavior on CeO_2-NPs. This experimental design is based on determining the coefficients that fit a polynomial function to describe the system under study and the influence of the proposed factors on the target function (Sánchez *et al.*, 2000). In this case, the phosphate adsorption percentage was selected as the objective function. As a secondary objective, the chemical surface and nanostructure changes during the adsorption-desorption process were studied by infrared attenuated total reflectance (ATR-IR), transmission electron microscopy (TEM), and high-resolution transmission electron microscopy (HRTEM).

MATERIALS AND METHODS

CeO_2 nanoparticle preparation

CeO_2 nanoparticles were synthesized in aqueous solution, using milli-Q grade water. All reagents were purchased from Sigma-Aldrich and used as received. Briefly, the CeO_2-NP synthesis was based on the methodology proposed by Zhang *et al.* (2004), from $Ce(NO_3)_3$ salt oxidized under basic pH conditions to Ce^{4+} using 0.5 M hexamethylenetetramine (HMT) .

Characterization and stability of nanoparticles

For full characterization of the NPs, the obtained nanoparticle suspension was analyzed using dynamic light scattering (DLS) to determine the nanoparticle size distribution in a Nanoparticles Analysis System (Malvern, UK). Zeta potential (ZP) measurements were also performed to study the surface properties and any changes after the experiments. X-Ray diffraction spectra (using a PANalytical X´Pert diffractometer with a Cu Kα radiation source) were obtained to determine the crystalline phase of the samples. TEM images of the samples

were also taken using a JEOL 1010 operating at an accelerating voltage of 80 kV after the nanoparticle synthesis to characterize the NPs before and after the phosphate adsorption-desorption process. The samples were ultrasonically suspended in ethanol and then dropped onto amorphous carbon specimen grids. HRTEM was used to analyze the CeO_2-NPs after the phosphate adsorption process. After the desorption treatment process with NaOH, the morphology, electron diffraction pattern, and the elemental analysis of the NPs were determined; the latter being performed by using energy dispersive X-ray spectroscopy (EDS). Inductively coupled plasma mass spectrometry (ICP-MS) using an Agilent Equipment (Model 7500ce) was used to analyze the initial and final phosphate concentration in solutions.

Table 1 and Fig. 1 show some of the main characteristics of the used nanoparticles as they were synthesized.

Adsorption-desorption study

A Box-Hunter spherical experimental design was used to study the influence on the adsorption behavior of the initial concentration of phosphate and CeO_2-NPs. In order to limit the range of the initial concentration of phosphate, the adsorption capacity of three initial phosphate concentrations (100, 50, 10 mg L^{-1}) were tested, while the concentration of CeO_2-NPs was maintained constant (320 mg L^{-1}) and the contact time was fixed at 24 hours to ensure that equilibrium conditions were reached. Previous experiments (data not shown) performed at 100 mg L^{-1} of phosphate and 320 mg L^{-1} of CeO_2-NPs showed that at 3 hours of contact time nearly 100% of the phosphate was adsorbed, and from this time phosphate was not detectable in solution. Once the range of the studied variables was limited, the ranges of the variables used in the Box-Hunter spherical method were: phosphate: 0-170 mg L^{-1}, CeO_2-NPs suspension 0-320 mg L^{-1}. These ranges cover the typical values found for phosphate concentration in most waters and wastewaters. The exact values used in the experiment are

presented in Table 2. The objective function of the experimental design was the removal percentage of phosphate from the solution. The experimental design was statistically validated by using the Sigmaplot 11.0 software package (Systat Software Inc, San Jose, USA), from four replicated experiments (Table 2).

The adsorption processes were performed as follows: Equal volumes of potassium phosphate solutions and CeO_2-NPs suspensions were poured into a vessel and stirred at 150 rpm at room temperature and pH 7 for 24 hours; the samples were separated by centrifugation (10000 g, 10 min) and the liquid-phase phosphate concentration was analyzed by using ICP-MS. The desorption study was performed using the same procedure used for adsorption, although only the concentrations of phosphate of 170 mg L^{-1} and CeO_2-NPs suspension of 320 mg L^{-1} were tested. The solid phases obtained after adsorption and centrifugation were dried at room temperature for 24 hours. In the same vessel the following solvents for desorption were used: deionized water, 0.1 M NaOH, and 0.5 M NaOH. The suspensions were stirred for 24 hours, separated by centrifugation (10000 g, 10 min), and the concentration of phosphate in the liquid phase determined. The initial and final concentrations of phosphate were again measured using ICP-MS. All desorption experiments were carried out in triplicate and the average values are presented. The standard deviation was very low for all experiments (< 5%) and is not presented.

RESULTS AND DISCUSSION

Synthesis of CeO_2 nanoparticles

Synthesized CeO_2 nanoparticles crystallize in a cubic fluorite structure (Fig. 1a) with the predominant crystallographic planes exposed at the (111) surface (Fig. 1b), which are responsible for the catalytic behavior (Zhang *et al.*, 2004). The average diameter obtained was

11.7 ± 1.6 nm (Fig. 1c). The size distribution was obtained after image analysis of different TEM images, by counting at least 500 NPs. These nanocrystals have more cerium atoms than oxygen atoms per unit surface; unlike (100)-terminated CeO_2-NPs, which are predominantly oxygen terminated (Trovarelli, 2002). This fact is related to the storage and release of oxygen and the promotion of noble-metal activity and dispersion (Stanek *et al.*, 2008). Both phenomena are controlled by the type, size, and distribution of oxygen vacancies as these are the most relevant surface defects (Carrettin *et al.*, 2004).

Adsorption-desorption study

The response of the objective function (percentage of phosphate removal) as a result of the initial phosphate and CeO_2-NPs concentrations was tested in the experimental design. The surface obtained fitted well with lineal equation such Eq. 1, where x and y are the normalized values of the factors considered:

$$F = y_o + ax + by \qquad \text{(Eq. 1)}$$

being $R^2 = 0.9803$, $y_o = 50.05$, $a = 0.227$ and $b = -0.313$.

The use of this experimental method permits to study the removal capacity of CeO_2-NPs using a relatively small number of experiments and provides a reliable tool to predict adsorption at any concentrations, being some values close to 100% removal (Table 2). This is an important advance since most of the studies published test randomly the effect of different parameters on the adsorption process and it has been validated in studies in different research areas (San Sebastián *et al*., 2003).

In relation to the adsorption capacities observed, they are within the range of 0.3-0.4 mg of phosphate per gram of CeO_2-NPs. In general, these values are higher than those found by other authors. Thus, Huang and Chiswell (2000) found a capacity of 0.30-0.33 mg phosphate per gram of air-dried spent alum, whereas other authors report the maintenance of

concentrations of total phosphorous using activated alumina columns (Donnert and Manfred, 1999).

Phosphate speciation can have an important role on the adsorption process. In this study, adsorption experiments were performed at pH 7. At this pH phosphate is mainly in the form of monovalent phosphate ($H_2PO_4^-$) and, in a minor amount, in the form of divalent phosphate (HPO_4^{2-}). According to Lin *et al.* (2011), the physical adsorption of phosphate onto active carbon is not pH-dependent. However, adsorption onto other surfaces, such as particles of $Al/SiO_2/Fe_3O_4$, was found to be clearly pH-dependent, being 4.5 the optimum pH for phosphate removal. In this case, the increase in the adsorption capacity was attributed to changes on the surface of $Al/SiO_2/Fe_3O_4$ particles and not due to changes in phosphate speciation. At acid pH the surface charge of cerium oxide nanoparticles is positive (Di *et al*., 2006), thus the adsorption capacity of phosphate at acid pH could be higher, although in this study we preferred to work under neutral pH, as it is more common in real waters. Additionally, according to Recillas *et al.* (2010), CeO_2 nanoparticles dissolve under acidic conditions.

Adsorption experiments were performed with the aim to recover both nanoparticles and the adsorbed material. Deionized water and NaOH (0.5 M and 0.1 M) were selected as solvents for desorption. The phosphate desorption percentages obtained were 27% and 8% for NaOH 0.5 M and 0.1 M, respectively, whereas deionized water did not produce any desorption at the evaluated concentrations. This opens the research on using effective solutions for desorbing valuable materials such as phosphate, which is a fundamental point for an economical and environmentally friendly overall process. In this sense, some authors have proved the recovery of high quality phosphate after the desorption process from wastewater (Ebie *et al*., 2008; Midorikawa *et al.*, 2008), although, to our knowledge, this process has not been tested using nanoparticles.

TEM and HRTEM

TEM images of CeO_2-$NPsPO_4$ and CeO_2-$NPsPO_4$-NaOH are shown in Fig. 2. The NPs obtained after the phosphate adsorption process show particles with a homogeneous size and similar irregular shape (Fig. 2a), whereas at higher amplification (Fig. 2b) the shape of the particles is roughly spherical. The estimated diameter of the NPs is around 12 nm (Fig. 2b). Changes in the morphology and size of the nanostructure were found after the desorption treatment with NaOH solutions. At low amplification a homogeneous material was observed (Fig. 2c), whereas at higher amplification fused elongated NPs were observed (Fig. 2d). The diameter of the fused particles is around 24 nm (Fig. 2d).

Fig. 3a shows the HRTEM images of NPs after adsorption treatment (CeO_2-$NPsPO_4$); these are mainly the NPs bounded by (111) planes. This result is expected because this plane is the most stable (Gross *et al.*, 1997). The lattice spacing as measured from the TEM image is approximately 0.32 nm for (111), in accordance with the expected fluorite structure, and can be described as a face-centered cubic packing of cations, with anions in all of the tetrahedral holes (the Ce^{4+} cation is surrounded by 8 O_2^- ions with each O_2^- coordinated to 4 Ce^{4+}). Fig. 3b shows the electron diffraction pattern of the CeO_2-$NPsPO_4$. The ring patterns confirm the nanocrystalline structure and are consistent with the indexed cubic cerium oxide with a fluorite structure. The four rings (from inner to outer) correspond to the (111), (200), (220), and (300) reflections. The most intense line arises from (111), which corresponds to a 0.54 nm lattice constant (calculated from the radii of Debye-Scherrer rings); this is expected for the fluorite structure of CeO_2 (Strom and Jun, 1980). After the desorption process (CeO_2-$NPsPO_4$-NaOH) the lattice spacing and the nanoparticle size remained unchanged (Fig. 3c).

The CeO_2-$NPsPO_4$ elemental analysis results showed the presence of Ce, O, P, Na, and K after the desorption process (Fig. 3d) and were compared with those of CeO_2-$NPsPO_4$-

NaOH. As expected, a decrease in the phosphate concentration and an increase in sodium concentration were observed.

CONCLUSIONS

The high capacity for phosphate adsorption at low and high concentrations found for CeO_2-NPs is a promising result for water and wastewater treatment processes. The use of a Box-Hunter spherical experimental design to study the adsorption process resulted in a better interpretation of the optimum conditions of adsorption than has been previously obtained, and with a relatively small number of experiments. During the phosphate adsorption and desorption processes several changes in the surface chemistry and morphology of NPs were observed.

Acknowledgements

Sonia Recillas thanks Universitat Autònoma of Barcelona for a post-doctoral fellowship.

References

Al-Abadleh, H. I. & Grassian, V. H. 2003. Oxide surfaces as environmental interfaces. *Surf. Sci. Rep.* **52**, 63-161.

Barnard, J. L. 1983. Design Consideration Regarding Phosphate Removal in Activated Sludge Plants. *Wat. Sci. Technol.* **15**, 319-328.

Blaney, L. M., Cinar, S. & SenGupta, A. K. 2007. Hybrid anion exchanger for trace phosphate removal from water and wastewater. *Water Res.* 41, 1603-1613.

Box, G. E. P., Hunter, W. G. & Hunter, J. S. 1978. Statistics for Experimenters, Wiley, NY.

Campbell, C. T. & Peden, C.H. 2005. Oxygen vacancies and catalysis on ceria surfaces. *Science* **309**, 713-714.

Carrettin, S., Concepción, P., Corma, A., López Nieto, J. M. & Puntes, V.F. 2004. Nanocrystalline CeO_2 Increases the Activity of Au for CO Oxidation by Two Orders of Magnitude. *Angew. Chem. Int. Ed.* **43**, 2538-2540.

Di, Z-C., Ding, J., Peng, X-J., Li, Y-H., Luan, Z-K., Liang, J. 2006. Chromium adsorption by aligned carbon nanotubes supported ceria nanoparticles. *Chemosphere* **62**, 861-865.

Donnert, D. & Salecker, M. 1999. Elimination of Phosphorus from Municipal and Industrial Waste Water. *Wat. Sci. Technol*. **40**, 195-202.

Ebie, Y., Kondo, T., Xu, K., Kadoya, N., Mouri, M., Maruyama, O., Noritake S. & Inamori Y. 2008. Recovery oriented phosphorus adsorption process in decentralized advanced Johkasou. *Wat. Sci. Technol*. **57**, 1977-1981.

Fernández, J., Ribas, J., Freixó, A. & Sánchez, A. 2003. Characterisation of phosphorous forms in wastewater treatment plants. *J. Hazard. Mater*. **97**, 193-205.

Gross, P. R., Matthew, L., Donald, E., Sparks, L., Goldberg, S. & Ainsworth, C. 1997. Arsenate and Chromate Retention Mechanisms on Goethite. 2. Kinetic Evaluation Using a Pressure-Jump Relaxation Technique. *Environ. Sci. Technol.* **31**, 321-326.

Huang, S.H. and Chiswell, B. 2000. Phosphate removal from wastewater using spent alum sludge. *Wat. Sci. Technol.* **42**, 295-300.

Lin, Y-F., Chen, H-W., Chang, C-C., Hung, W-C., Chiou C-S. 2011. Application of magnetite modified with aluminum/silica to adsorb phosphate in aqueous solution. *J. Chem. Technol. Biotechnol.* **86**, 1449-1456.

Midorikawa, I., Aoki, H., Omori, A., Shimizu, T., Kawaguchi, Y., Kassai, K. & Murakami, T. Recovery of high purity phosphorus from municipal wastewater secondary effluent by a high-speed adsorbent. 2008. *Wat. Sci. Technol.* **58**, 1601-1607.

Nowack, B. & Stone, A. T. 2006. Competitive adsorption of phosphate and phosphonates onto goethite. *Water Res.* **40**, 2201-2209.

Ozacar, M. 2003. Adsorption of phosphate from aqueous solution on to alunite. *Chemosphere* **51**, 321-327.

Peng, X., Luan, Z., Ding, J., Di, Z., Li, Y. & Tian, B. 2005. Ceria nanoparticles supported on carbon nanotubes for the removal of arsenate from water. *Mater. Lett.* **59**, 399-403.

Recillas, S., Colón, J., Casals, E., González, E., Puntes, V., Sánchez, A & Font, X. 2010. Chromium VI adsorption on cerium oxide nanoparticles and morphology changes during the process. *J. Hazard. Mater.* **184**, 425-431.

San Sebastián, N., Fíguls, J., Font, X. & Sánchez, A. 2003. Pre-oxidation of an extremely polluted industrial wastewater by the Fenton's reagent. *J. Hazard Mater*. **101**, 315-322.

Sánchez, A., Río, J.L., Valero, F., Lafuente, J. Faus, I. & Solà, C. 2000. Continuous enantioselective esterification of trans-2-phenyl-1-cyclohexanol using a new *Candida rugosa* lipase in a packed bed bioreactor. *J. Biotechol.* **84**, 1-12.

Scheer, H. & Seyfried, C. F. 1997. Enhanced biological phosphate removal: modelling and design in theory and practice. *Wat. Sci. Technol*. **35**, 43-52

Stanek, C. R., Tan, A. H. H., Owens, S. L. & Grimes, R.W. 2008. Atomistic simulation of CeO_2 surface hydroxylation: implications for glass polishing. J. *Mater. Sci.* **43**, 4157-4162.

Strom Jr, J.G. & Jun, H. 1980. Kinetics of hydrolysis of methenamine. *J. Pharm. Sci.* **69**, 1261-1263.

Trovarelli, A. 2002. Catalysis by Ceria and related materials, Imperial College Press, London.

Xiao, H. I., Ai, Z. H. & Zhang, L.Z. 2009. Non-aqueous Sol-Gel synthesized hierarchical CeO_2 nanocrystal microspheres as novel adsorbents for wastewater treatment. *J. Phys. Chem.* C. **113**, 16625-16630.

Xu, K., Deng, T., Liu, J. & Peng, W. 2010. Study on the phosphate removal from aqueous solution using modified fly ash. *Fuel* 89, 3668-3674.

Yuan, Q., Duan, H., Li, L., Sun, L. D., Zhang, Y. W. & Yan, C.H. 2009. Controlled synthesis and assembly of ceria-based nanomaterials. *J. Colloid Interf. Sci.* **335**, 151-167.

Zhang, F., Jin, Q. & Chan, S. W. 2004. Ceria nanoparticles: Size, size distribution, and shape. *J. Appl. Phys.* **95**, 4319-4327.

Tables

Table 1. Main characteristics of the CeO_2 nanoparticles used. Values presented were obtained as nanoparticles were synthesized.

Nanoparticle	**CeO_2**
Concentration (mg mL^{-1})	0.64
Approximate number of NPs (NPs mL^{-1})	~10^{16}
Mean size (nm)	12
Shape	spherical
Zeta potential (mV)	+11.5
Stabilizer*	HMT
Stabilizer concentration (mM)	8.3
pH (original)	9
Estimated surface area (m^2 g^{-1})	121

*HMT: Hexamethylenetetramine

Table 2: Tested conditions according to the Box-Hunter experimental design matrix. Results of objective function (percentage removal of phosphate after adsorption) are also presented, being x and y are the normalized factors considered in the experimental design.

Sample	CeO_2-NPs (mg L^{-1})	Phosphate (mg L^{-1})	CeO_2-NPs (x normalized)	Phosphate (y normalized)	Phosphate removal (%)
1	170	100	0	0	56.9
2	170	100	0	0	55.3
3	170	100	0	0	56.1
4	170	100	0	0	57.2
5	20	100	-1	0	13.7
6	320	100	1	0	96.9
7	170	10	0	-1	84.7
8	170	190	0	1	31.7
9	75	164.5	-0.71	0.71	19.3
10	275	164.5	0.71	0.71	58.0
11	75	35.5	-0.71	-0.71	66.8
12	275	35.5	0.71	-0.71	95.7

Figures

Figure 1. Cerium oxide NPs: a) TEM image; b) X-ray diffraction spectra; c) size distribution.

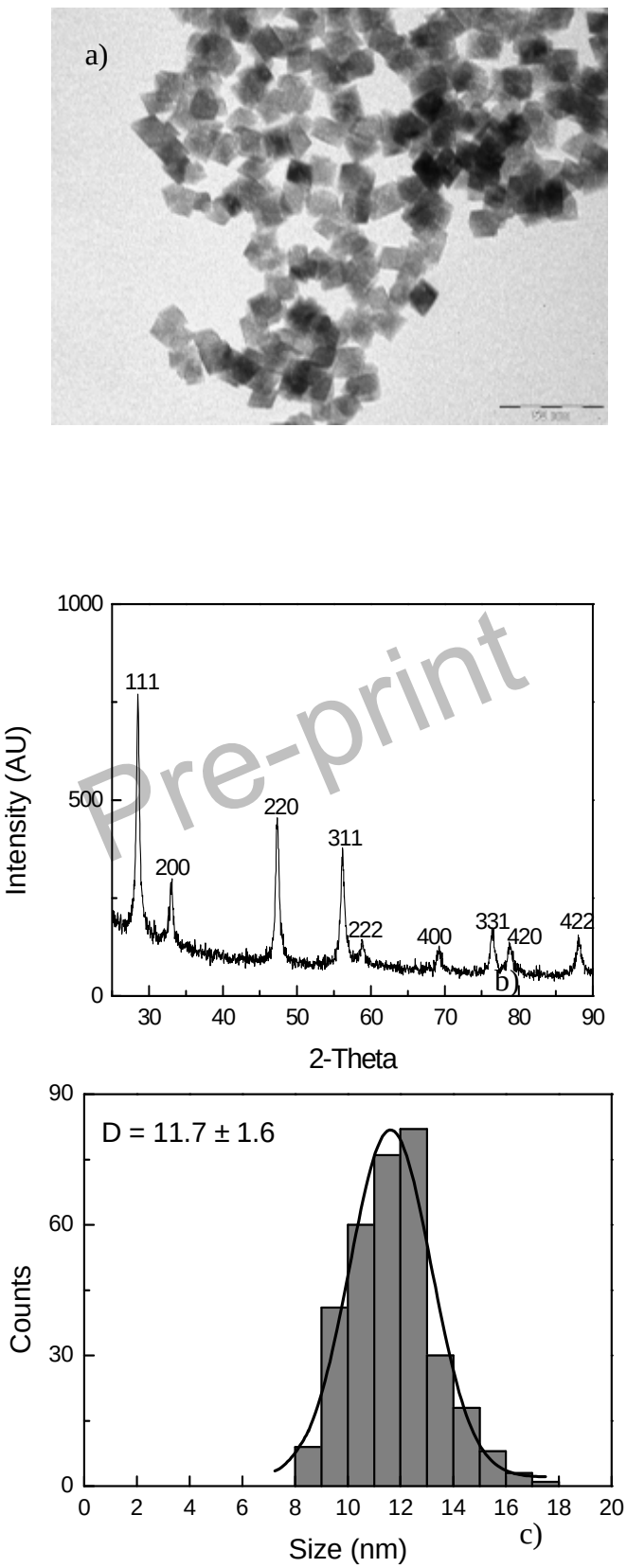

Figure 2. TEM images of: a-b) CeO_2 nanoparticles after phosphate adsorption (CeO_2-$NPsPO_4$); c-d) CeO_2 nanoparticles after the desorption process (CeO_2-$NPsPO_4$-NaOH).

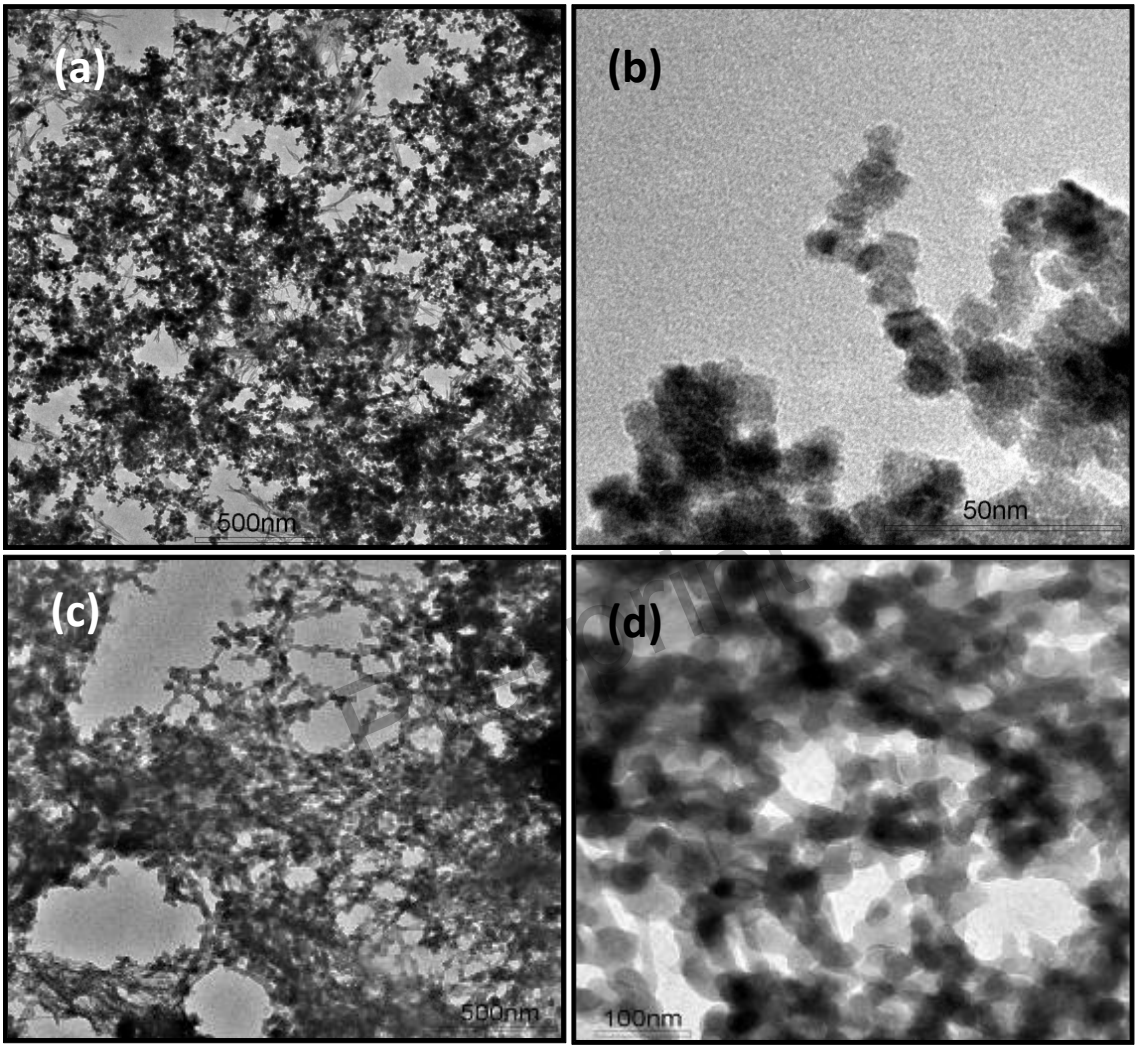

Figure 3. HRTEM images of CeO_2-NPs: a) with phosphate adsorbed; b) electron diffraction pattern of CeO_2-NPs with phosphate adsorbed; c) CeO_2-NPs after desorption process and d) elemental analysis of CeO_2-NPs after phosphate adsorption (CeO_2-NPsPO_4) and after the desorption process (CeO_2-NPsPO_4-NaOH).

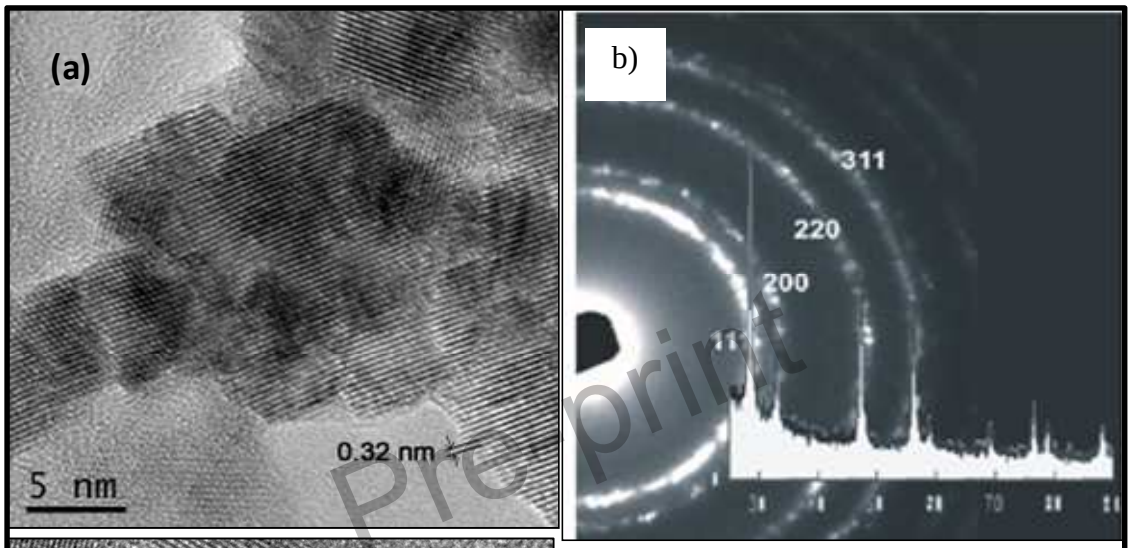

d)

Element	CeO_2-PO_4-NaOH (%Atomic)	CeO_2-PO_4 (%Atomic)
C	0.00	0.00
O	48.56	49.80
Na	12.64	0.00
P	1.62	5.24
K	3.58	0.00
Cu	0.00	0.00
Ce	33.60	44.95